13

Nonlinear Heat Transfer Modeling

Jan Lienemann[1], Amirhossein Yousefi[2], and Jan G. Korvink[1]

[1] Institute for Microsystem Technology, Albert Ludwig University
Georges Köhler Allee 103, 79110 Freiburg, Germany
{lieneman,korvink}@imtek.de
[2] Lehrstuhl für Regelungstechnik, Technische Universität München,
Boltzmannstr. 15, D-85748 Garching bei München, Germany
Yousefi@tum.de

Summary. The simulation of heat transport for a single device is easily tackled by current computational resources, even for a complex, finely structured geometry; however, the calculation of a multi-scale system consisting of a large number of those devices, e.g., assembled printed circuit boards, is still a challenge. A further problem is the large change in heat conductivity of many semiconductor materials with temperature. We model the heat transfer along a 1D beam that has a nonlinear heat capacity which is represented by a polynomial of arbitrary degree as a function of the temperature state. For accurate modeling of the temperature distribution, the resulting model requires many state variables to be described adequately. The resulting complexity, i.e., number of first order differential equations and nonlinear parts, is such that a simplification or model reduction is needed in order to perform a simulation in an acceptable amount of time for the applications at hand.

In this paper, we describe the modeling considerations leading to a large nonlinear system of equations. Sample results from this model and examples of successful model order reduction can be found in [YLLK04] and the corresponding benchmark document, available online on the Oberwolfach Model Reduction Benchmark Collection website [OBC] ("Nonlinear heat transfer modeling").

13.1 Modeling

We model the heat transfer along a 1D beam with length L, cross sectional area A and nonlinear heat conductivity κ. The heat conductivity is represented by a polynomial in temperature $T(x,t)$ of arbitrary degree n

$$\kappa(T) = a_0 + a_1 T + \cdots + a_n T^n = \sum_{i=0}^{n} a_i T^i. \tag{13.1}$$

The right end of the beam (at $x = L$) is fixed at ambient temperature. The model features two inputs, a time-dependent uniform heat flux f at the left

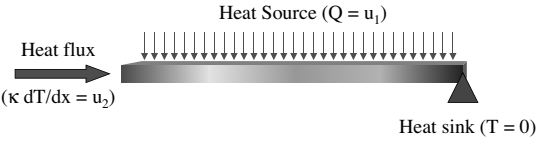

Fig. 13.1. The modeled beam with heat flux inputs and heat sink.

end (at $x = 0$) and a time dependant heat source Q along the beam. We denote the beam volume where we wish to solve the equations by Ω.

By including (13.1) in the differential form of the heat transfer equation,

$$-\nabla \cdot (\kappa(T)\nabla T) + \rho c_p \dot{T} = Q, \tag{13.2}$$

we obtain the following expression,

$$-\sum_{i=0}^{n} a_i \nabla \cdot \left(T^i \nabla T\right) + \rho c_p \dot{T} = Q, \tag{13.3}$$

where ρ is the density and c_p is the heat capacity, which are both assumed to be constant for the considered temperature range. This approximation can be justified from measurements of semiconductors, which show that the temperature dependency of c_p is much smaller than that of κ. This rapid change is a result of the special band structure of the material. It follows an exponential law:

$$\kappa = \kappa_0 \mathrm{e}^{\alpha(T-T_0)}. \tag{13.4}$$

The heat capacity for silicon changes from 1.3 to 2 in the temperature range of 200 to 600 Kelvin, while κ changes from 280 W/m K to 60 W/m K.

13.1.1 Finite Element Discretization

Following the Ritz-Galerkin finite element formulation, we require orthogonality with respect to a set of test functions $N_k(x)$, $k = 1, \ldots, N$:

$$-\sum_{i=0}^{n} a_i \int_\Omega N_k \nabla \cdot \left(T^i \nabla T\right) \mathrm{d}\Omega + \int_\Omega N_k \rho c_p \dot{T} \mathrm{d}\Omega = \int_\Omega N_k Q \mathrm{d}\Omega \quad \forall N. \tag{13.5}$$

By using the Green-Gauß theorem, we get the weak form

$$\begin{aligned} \sum_{i=0}^{n} a_i \int_\Omega \nabla N_k T^i \nabla T \mathrm{d}\Omega - \int_{\partial\Omega} \underbrace{\kappa(T)\nabla T \cdot \mathbf{n}}_{J} N_k \mathrm{d}\partial\Omega + \int_\Omega N_k \rho c_p \dot{T} \mathrm{d}\Omega \\ = \int_\Omega N_k Q \mathrm{d}\Omega, \end{aligned} \tag{13.6}$$

where a positive J denotes a heat flux into one end of the beam. We approximate the temperature profile by shape functions

$$T(x) = \sum_{j=1}^{N} T_j N_j(x), \tag{13.7}$$

which are the same as the test functions N_k and, after moving all inputs to the right side, obtain

$$\begin{aligned} \sum_{i=0}^{n} a_i \sum_{j=1}^{N} T_j \int_\Omega \nabla N_k T^i \nabla N_j \mathrm{d}\Omega + \rho c_p \sum_{j=1}^{N} \dot{T}_j \int_\Omega N_k N_j \mathrm{d}\Omega \\ = Q \int_\Omega N_k \mathrm{d}\Omega + J \int_{\partial\Omega} N_k \mathrm{d}\partial\Omega. \end{aligned} \tag{13.8}$$

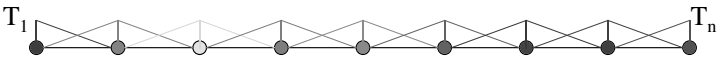

Fig. 13.2. Linear shape functions for FEM discretization

The second, third and fourth term in this equation are linear and yield a constant mass matrix M and a scattering matrix B on the right side to distribute the two inputs J and Q to the load vector. For a linear 1D beam element e of length l with nodes m and $m+1$, we have the element contributions

$$\mathsf{M}_e = \begin{bmatrix} 2/3 & 1/6 \\ 1/6 & 2/3 \end{bmatrix}, \quad \mathsf{B}_e = \begin{bmatrix} 0 & Al/2 \\ 0 & Al/2 \end{bmatrix} \tag{13.9a}$$

except for the leftmost element, where

$$\mathsf{B}_1 = \begin{bmatrix} A & Al/2 \\ 0 & Al/2 \end{bmatrix}. \tag{13.9b}$$

When using linear shape functions, the gradients are constant. The element stiffness matrix then reads

$$\mathsf{A}_e = \sum_{i=0}^{n} a_i \frac{A}{l^2} \int_0^l \left(T_m(1 - x/l) + T_{m+1} x/l\right)^i \mathrm{d}x \begin{bmatrix} 1 & -1 \\ -1 & 1 \end{bmatrix} \tag{13.10a}$$

$$= \sum_{i=0}^{n} a_i \frac{A}{l} \frac{T_{m+1}^{i+1} - T_m^{i+1}}{(i+1)(T_{m+1} - T_m)} \begin{bmatrix} 1 & -1 \\ -1 & 1 \end{bmatrix}. \tag{13.10b}$$

For $i > 0$, this yields a nonlinear stiffness matrix, while for $i = 0$ after performing the multiplication of the matrix A with $\mathbf{x}$, the denominator is constant. We introduce a vector $\mathbf{f}(T)$ on the right side which collects all nonlinear parts of the discretized equation:

$$\mathsf{A}_{\text{linear}} \mathbf{T} + \rho c_p \mathsf{M} \dot{\mathbf{T}} = \mathsf{B} \begin{pmatrix} J \\ Q \end{pmatrix} + \mathbf{f}(\mathbf{T}). \tag{13.11}$$

To move the nonlinear terms in (13.10b) to the right side, we multiply them with $T_m - T_{m+1}$ and subtract them from both sides of the equation. Every element e contributes two entries to the vector $\mathbf{f}(T)$:

$$\mathbf{f}_e = \sum_{i=1}^{n} a_i \frac{A}{l} \frac{T_{m+1}^{i+1} - T_m^{i+1}}{i+1} \begin{pmatrix} 1 \\ -1 \end{pmatrix}. \tag{13.12}$$

We observe that the nonlinearities are polynomial.

We then denote $\mathsf{E} = \rho c_p \mathsf{M}$ and introduce a gather matrix C which returns some linear combinations of the degrees of freedom (or more often, selects some single DOFs) which are the most interesting for the application. In this particular example, C is a row vector with 1 at the first position, 1 at the entry in the middle ($\lceil n/2 \rceil$) and 0 everywhere else. This returns the temperatures at the leftmost end (where the heat flux is applied) and in the middle of the beam.

After renaming $\mathbf{T}$ to $\mathbf{x}$ to comply with the DSI file format specifications described in Chapter 12, we end up with the following system of equations:

$$\mathsf{E}\dot{\mathbf{x}} + \mathsf{A}\mathbf{x} = \mathsf{B}\mathbf{u} + \mathsf{F}\mathbf{f}(\mathbf{x}, u) \tag{13.13}$$

$$\mathbf{y} = \mathsf{C}\mathbf{x} \tag{13.14}$$

13.1.2 Implementation

The scheme above was implemented in the computer algebra system *Mathematica* [Mat]. *Mathematica*'s symbolic capabilities allow for an easy implementation of vectors of nonlinear functions. The data is then exported to a file in the DSI format; see Chapter 12. We have also created an interactive web application which allows one to specify the parameters of the model for customized matrix generation, available on [Mst].

A number of linear and nonlinear precomputed examples are available from the benchmark.

13.2 Discussion and Conclusion

A general model for the heat conduction with temperature dependent heat conductivity in a 1D beam was developed. It is possible to include polynomial nonlinearities with an arbitrary polynomial degree. The effects of nonlinearities are clearly visible from simulation results.

13.3 Acknowledgments

This work was supported by Deutsche Forschungsgemeinschaft (DFG) project MST-Compact under contract numbers KO-1883/6 and LO 408/3-1 and by an operating grant of the University of Freiburg.

References

[YLLK04] Yousefi, A., Lienemann, J., Lohmann, B., Korvink, J.G.: Nonlinear Heat Transfer Modelling and Reduction. In: Proceedings of the 12th Mediterranean Conference on Control and Automation, Kusadasi, Aydin, Turkey, June 6–9 (2004)

[OBC] http://www.imtek.uni-freiburg.de/simulation/benchmark/

[Mst] http://www.imtek.uni-freiburg.de/simulation/mstkmpkt.

[Mat] http://www.wolfram.com.